SAND2015-9788C

# Determining Model Form Uncertainty of Reduced Order Models

Matthew S. Bonney
Ph.D. Student
University of Wisconsin-Madison
Madison, WI
msbonney@wisc.edu

Daniel C. Kammer
Professor
University of Wisconsin-Madison
Engineering Physics
Madison, WI
kammer@engr.wisc.edu

Matthew R.W. Brake
Sandia National Laboratories*
Albuquerque, NM
mrbrake@sandia.gov

## ABSTRACT

The quantification of model form uncertainty is very important for engineers to understand when using a reduced order model. This quantification requires multiple numerical simulations which can be computationally expensive. Different sampling techniques, including Monte Carlo and Latin Hypercube, are explored while using the maximum entropy method to quantify the uncertainty. The maximum entropy method implements random matrices that maintain essential properties. This is explored on a planar frame using different types of substructure representations, such as Craig-Bampton. Along with the model form uncertainty of the substructure representation, the effect of component mode synthesis for each type of substructure representation on the model form uncertainty is studied.

**Keywords**: Model-Form Uncertainty, Uncertainty Quantification, Maximum Entropy, Sub-structuring

## 1 Introduction

Model form uncertainty is a very important research topic in the study of computational mechanics. Depending on how the analyst choses to represent the material or structure, the results from the simulations may differ. One major cause of this difference is model reduction. High-fidelity models can give high accuracy results although the computational time and resources is expensive. To reduce the cost of this computational requirement, a model reduction is typically used. This reduction induces some model form error, which can be difficult to quantify.

The study of model reduction uncertainty due to truncation has typically been done by calculating a percent difference in the natural frequency individually. This gives first order uncertainty information that cannot be propagated into assembled system if sub-structuring is used. In order to perform an uncertainty propagation, information about the model itself is required on a physical level, such as mass and stiffness matrices. The method used to describe the uncertainty in the system matrices is the maximum entropy approach [2, 3, 4, 5, 6]. This method, primarily developed by Soize, incorporates the use of random matrix theory. The maximum entropy approach is able to characterize the uncertainty of the physical matrices in terms of a scalar value for each system matrix. This scalar

*Sandia National Laboratories is a multi-program laboratory managed and operated by Sandia Corporation, a wholly owned subsidiary of Lockheed Martin Corporations, for the U.S. Department of Energy's National Nuclear Security Administration under Contract DE-AC04-94AL85000.

value is used to characterize the randomness of the system matrix which is simple to propagate to a desired result using sampling methods such as Monte-Carlo (MC). Maximum entropy uses the probability from the MC analysis instead of a percentage difference of deterministic frequencies. This technique is used on a Craig-Bampton (CB) [7] reduced order model (ROM).

# 2 Theory

This research combines a model reduction technique, CB, and a method for determining the uncertainty of the physical system matrices, maximum entropy. Craig-Bampton is a technique that have been thoroughly studies and understood for the past 40 years [7]. The maximum entropy approach used in this paper is a relatively new technique for quantifying the error associated with the system matrices first described in [3] and further in [5]. The exact method used in this paper is described in detailed in [6]. Each of these techniques are explained in the next sections.

## 2.1 Craig-Bampton/Fixed Interface

Craig-Bampton is a model reduction technique that uses fixed interface modes along with physical interface DOF. The fixed interface modes are truncated typically based on frequency. The reduction can be written as

$$\begin{pmatrix} u_i \\ u_j \end{pmatrix} = \begin{bmatrix} \Phi_k & \Psi \\ 0 & I \end{bmatrix} \begin{pmatrix} \eta_k \\ u_j \end{pmatrix}, \tag{1}$$

where $u$ are the physical DOF, $\Phi$ are the fixed-interface modes, $\Psi$ are the constraint modes that describe how the interior DOF deflect due to a unit displacement in a single interface DOF, and $\eta$ are the fixed-interface modal DOF. 0 is a matrix of zeros, $I$ is the identity matrix, the subscript $i$ is the interior DOF, subscript $j$ is the interface DOF, and the subscript $k$ is the kept fixed-interface mode. The fixed-interface modes are typically truncated at frequencies greater than 1.5 or 2 times the highest desired frequency. This reduction is done for each substructure. Once this reduction is performed, the system matrices are combined and synthesized. The system DOF are organized for two substructures, as is the form of this investigation's problem, as

$$u_{cb} = \begin{pmatrix} \eta_k^\alpha \\ u_j^\alpha \\ \eta_k^\beta \\ u_j^\beta \end{pmatrix}, \tag{2}$$

where the superscript $\alpha$ refers to the first substructure and the superscript $\beta$ refers to the second substructure. This partitioning of the DOF for this synthesis yields system matrices in the form of

$$[M_{cb}] = \begin{bmatrix} [M]^\alpha & 0 \\ 0 & [M]^\beta \end{bmatrix} \qquad [K_{cb}] = \begin{bmatrix} [K]^\alpha & 0 \\ 0 & [K]^\beta \end{bmatrix}. \tag{3}$$

The individual substructure matrices are already reduced by using the CB method. These system matrices form the equations of motion for an undamped and unforced system as

$$[M_{cb}]\ddot{u}_{cb} + [K_{cb}]u_{cb} = 0. \tag{4}$$

These subsystems are still independent and are not constrained together. The interface DOF are constrained to be equal. This is written as

$$u_j^\alpha = u_j^\beta = u_j. \tag{5}$$

This constraint reduces the DOF vector to

$$u = \begin{pmatrix} \eta_k^\alpha \\ \eta_k^\beta \\ u_j \end{pmatrix}. \tag{6}$$

The advantage of using this reduction is that the interface DOF are preserved in the substructure allowing for easy connection. The synthesized system contains the fixed interface modes from both substructures and the physical DOF at the interface. One disadvantage of using this ROM is for systems with highly connected interfaces. This type of system produces a relatively large ROM, which decreases the utility of this technique.

## 2.2 Maximum Entropy

The equations of motion of the system is based on linear mass and stiffness. The mass matrix is positive definite while the stiffness matrix is either positive definite or semi-positive definite depending if the system is constrained or contains rigid body motion. Due to the definiteness of the matrices, these can decomposed using a Cholesky decomposition similar to

$$[M] = [L_M]^T [L_M], \tag{7}$$

with $[L_M]$ is an upper triangular matrix that is the Cholesky decomposition of the mass matrix $[M]$. For a non-singular matrix, $[L_M]$ is a square matrix, and for a singular matrix, $[L_M]$ is a rectangular matrix. The Cholesky decomposition is a function of the input parameters to the finite element model. To incorporate model form error, a random germ is added which is also generated to be positive definite so that the resulting matrix is still positive definite or positive semi-definite. The germ is incorporated using the relation

$$[M] = [L_M]^T [G(\delta_M)][L_M], \tag{8}$$

where $[G]$ is a random germ with an expected value of $I$ and $\delta_M$ is the dispersion parameter for the mass matrix. The variance of the random germ is a function of $\delta$ scaled by the size of the matrix. More detail of how to formulate this germ is given in [1, 2, 3, 6]. The dispersion parameter is chosen to best fit the truth data, which corresponds to having the highest probability in the probability density function. Truth data can be given as many things such as the frequency response function, mode shapes, or natural frequencies. This research uses the first 11 elastic natural frequencies as the truth data. The probability is best given as the likelihood function, which is the objective function for the dispersion variable. The main calculation is the likelihood value for each dispersion variable which controls the variance of the random matrices. The likelihood value is defined as the joint probability that the truth data exists within the model. This is shown as

$$L(\delta) = \Pr(TruthData|\delta), \tag{9}$$

where $L(\delta)$ is the likelihood value and $Pr()$ is the probability value that the truth data exists in the model. For the simplicity of calculations, each natural frequency is treated as independent. Due to the independence, the joint probability can be rewritten as

$$\Pr(TruthData|\delta) = \Pi_i \Pr(\omega_i|\delta). \tag{10}$$

This calculation yields a value on the range of $[0, 1]$. The optimal dispersion value is defined as the argument maximum of the likelihood function. Since this calculation has a very small range, the differences between each dispersion value can be small which can be affected by the computer resolution error. In order to reduce this error, the log-likelihood function is used. For this calculations, the negative log-likelihood function is used in order to possibly use optimization techniques. The negative log-likelihood is calculated by computing $\ell = \sum_i -log(\Pr(\omega_i|\delta))$. The reason this works is because $-log$ is a monotonically decreasing function, which means that the argument minimum of the negative log-likelihood is the same as the argument maximum of the likelihood function.

The calculation of the likelihood is based on the probability measure. There are two ways to compute this probability: analytically or numerically. In order to calculate the probability analytically, the distribution of the natural frequency must be known which is very hard to generate. This simulation calculates the probability numerically based on a MC simulation. In order to calculate the probability, a histogram is used. For these calculations the tolerance band is based on 0.1% of the natural frequency. The probability is calculated as the percentage of the number of times a natural frequency lands within this tolerance band. The determination of the band is very critical in the execution of this analysis. A band that is too small will result in very large variability, while a band that is too large will not be able to differentiate between different dispersion values. The argument minimum of this negative log-likelihood function is the statistical estimate of the dispersion variable.

In this paper, the likelihood is computed with 5000 samples from a distribution and is run 50 times to show randomness of the likelihood. This permits the calculation of the empirical negative log-likelihood using the expression

$$EL(\delta) = \sup_i \ell_i(\delta), \tag{11}$$

in which, $i$ is the independent evaluation of the negative log-likelihood, $\ell_i$. This empirical formulation accounts for the randomness in the Monte-Carlo sampling technique. The optimal dispersion parameter is then chosen based on

$$\delta^{optimal} = \arg min\ EL(\delta). \tag{12}$$

The optimal dispersion parameter is used in a forward propagation of the matrices to determine the distribution of the desired output, such as reliability measure or dynamic characteristics.

# 3 Example System

The system used to illustrate these techniques is a planar fame with an appendage. This system is shown in Figure 1.

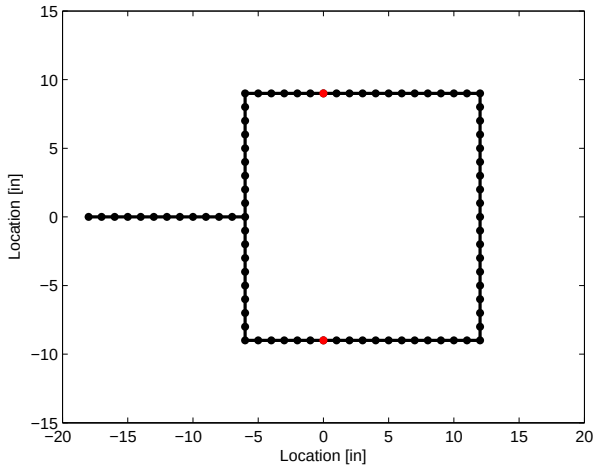


Figure 1: Planar Frame Example System

Figure 1 contains two subsystems that are combine to form the full system separated by the red nodes. The subsystem to the right is called system "B" and the subsystem to the left with the appendage is called system "D". These subsystems are reduced using the desired ROM technique, then are combined using component mode synthesis. Due to time constraints, only the synthesis of CB to CB is examined. The red connection nodes are shared between the two subsystems and are defined as the interface. The nodes shown in Figure 1 are connected using simple Euler beam elements. Each of the two subsystems has 129 degrees of freedom. This system is relatively small but large enough to show the complexity of the techniques and how they can be applied to larger systems.

The simulations are based on matching both the substructure and system frequencies for the first 11 elastic free-free modes. For subsystem B, the $11^{th}$ natural frequency is 4656.4 Hz and subsystem D has an eleventh natural frequency at 5511.5 Hz. The full system has an $11^{th}$ natural frequency of 1864.3 Hz. This selection of the first 11 elastic free-free modes was due to the idea that the higher frequency modes are more subject to model form error.

# 4 Results

## 4.1 Craig-Bampton Substructure

The first result is the analysis of a single substructure. This analysis took the first 11 elastic free-free modes for each substructure as the truth data. For both of the subsystems, the eleventh free-free frequency occurs at approximately the eleventh fixed-interface frequency. Typically, the modes kept in the reduction are any modes that have a frequency less than one and half to two times the highest desired frequency. For system B, the largest desired frequency is 4656.4 Hz so typically all the fixed-interface modes with frequency less than 7000 or 9300 Hz are kept. This would involve 15 or 18 fixed-interface modes. A sweep of the number of fixed-interface modes from 11 to 20 is performed to analyze the convergence of the dispersion parameter. This dispersion parameter has a maximum value of one when the size of the matrix goes to infinity. Due to this bound, the dispersion parameter is typically represented as a percentage. The Monte-Carlo analysis is performed on both systems for this range of kept fixed-interface modes with 5000 samples and performed 50 times to evaluate the empirical likelihood. In order to produce a single value for the dispersion parameter, only the stiffness of the system is chosen to be stochastic and the mass matrix is chosen to be

deterministic. This goes under the assumption that the mass and moments of inertia are accurately represented by Euler beam elements. These optimal parameters are shown in Table 1. The values in Table 1 highlighted in yellow represent keeping all modes less than one and a half times the eleventh free-free frequency and the values highlighted in green represent keeping all modes less than twice the eleventh free-free frequency.

Table 1: Optimal Substructure Dispersion Parameter

| # of Elastic Fixed-Interface Modes | $\delta_k$ for System B [%] | $\delta_k$ for System D [%] |
|---|---|---|
| 11 | 0.85 | 1.44 |
| 12 | 0.82 | 1.93 |
| 13 | 0.56 | 1.23 |
| 14 | 0.47 | 1.04 |
| 15 | 0.35 | 0.96 |
| 16 | 0.25 | 0.52 |
| 17 | 0.25 | 0.45 |
| 18 | 0.00 | 0.35 |
| 19 | 0.00 | 0.32 |
| 20 | 0.00 | 0.31 |

Some differences between the two substructures can be seen in Table 1. The first difference is that system D has a larger dispersion parameter for each case tested. This is believed to be due to the appendage on system D. The appendage creates modes that are harder to express in terms of fixed-interface modes. The general trend of these dispersion parameters follows the expected trend. The dispersion parameter goes to zero as more modes are included. One abnormality found was for system D. As the number of fixed-interface modes increases from 11 to 12, the dispersion parameter increases. These values are evaluated several times to verify that this is not caused by numerical issues and is uncertain as to the cause of this increase.

## 4.2 Craig-Bampton Combined System

The combination of the substructure into one system is a very typical utilization of this reduced order model technique. One major problem with doing a component mode synthesis on a system is that the uncertainty of the combined system is difficult to determine based on the uncertainty of the substructures. One difficulty is that the truth data for each system is different. Even if the frequencies used are similar, the mode shapes are different and are more difficult to express. The first result from the combined system is to try to find a relationship between the dispersion parameter of the substructures and the dispersion parameter of the combine system. This is expressed as taking the data from the previous section and finding the dispersion parameter of the system for the prescribed number of modes kept. The results of the dispersion parameter are shown in Figure 2.

The same basic trend that is found in Table 1 is found in Figure 2. As more modes are added, the dispersion parameter decreases. One interesting aspect is when 11 fixed-interface modes are kept for both of the substructures. The synthesized system has a dispersion parameter less than the dispersion parameter of either substructure. System B has a dispersion parameter of 0.85%, system D has a dispersion parameter of 1.44% and the synthesized system E has a dispersion parameter of 0.49%.

The number of modes shown in Figure 2 is not typical for a substructuring analysis. As mentioned, typical analysis uses one and a half or two times the highest frequency of the full system. System E has a highest frequency of interest of 1864.3 Hz so each substructure modes up to 2800 or 3700 Hz are kept. For the case of one and a half times, substructure B keeps 8 fixed-interface modes and substructure D keeps 6 fixed-interface modes. Using these modes, system E has a dispersion parameter of 1.97%. If twice the highest frequency is kept, substructure B keeps 9 modes and substructure D keeps 7 modes. This results in a dispersion parameter of 1.56% for system E. This shows increasing the amount of modes by one for each substructure creates a decrease in the dispersion parameter by 20%.

The determination of the dispersion of a synthesized system from the dispersion parameters of the substructures is a difficult analysis. One major difficulty is a theoretical issue that the truth data for the substructure and full structure are different. The chosen fact that eleven elastic free-free modes for both the substructure and full structure

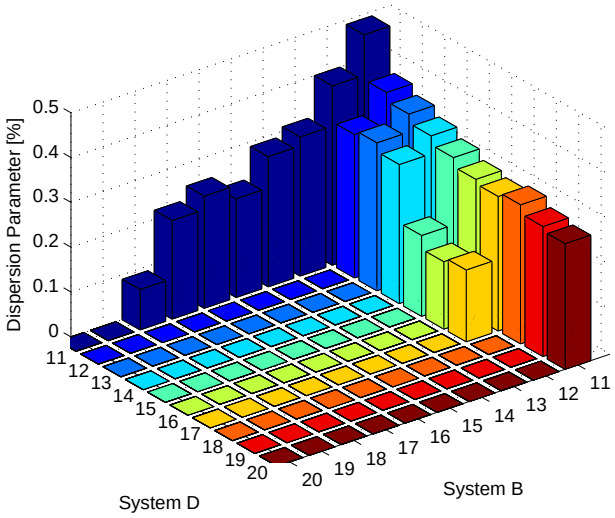


Figure 2: Synthesized System Dispersion Parameters

still contains different modes of vibration and do not represent the same information. The other difficulty is the piece-wise results. In figure 2, it is seen that if system B has at least 13 and system D has at least 12 fixed-interface modes, system E has a dispersion parameter of 0.00%. The cause of this is unknown and is currently being studied.

# 5 Conclusions

Uncertainty of a substructure can be quantified by many different methods. Using a dispersion parameter for a random matrix allows for a physical representation that encompasses the model form error. This formulation of model form error is developed by Soize. These random matrices are propagated using a Monte-Carlo analysis along with truth data to select an optimal dispersion parameter to contain the truth data with the highest probability. This was performed on a Craig-Bampton ROM. The expected trend for the CB ROM is that as more modes are included in the ROM, the uncertainty decreases is verified using a Monte-Carlo simulation. Two CB ROMs are also combined together to get a grasp on how the substructure uncertainty propagates into the assembled system. This research shows that using the rule of thumb gives the dispersion value of 2% to 1.5%. This research is a preliminary analysis on characterizing different ROMs. The use of dispersion parameters to describe the model form error allows for a single value to represent an entire system.

# References

[1] Batou A., Soize C., and Audebert S. Model identification in computational stochastic dynamics using experimental modal data. *Mechanical Systems and Signal Processing*, 50-51:Pages: 307–322, 2014.

[2] Robertson B.A., Bonney M.S., Gastaldi C., and Brake M.R.W. Quantifying epistemic and aleatoric uncertainty in the ampair 600 wind turbine. *Proceedings of the 33rd International Modal Analysis Conference*, 2014.

[3] Soize C. Maximum entropy approach for modeling random uncertainties in transient elastodynamics. *Journal of Acoustical Society of America*, 5:1979–1994, 2001.

[4] Soize C. Random matrix theory for modeling uncertainties in computational mechanics. *Computer Methods in Applied Mechanics and Engineering*, 194:1333–1366, 2004.

[5] Soize C. Generalized probabilistic approach of uncertainties in computational dynamics using random matrices and polynomial chaos decompositions. *International Journal for Numerical Methods in Engineering*, pages 1–32, 2009.

[6] Bonney M.S. and Brake M.R.W. Utilizing soize's approach to idetify parameter and model uncertainties. Technical Report SAND2014-19209, Sandia National Laboratories, Albuquerque, NM, 2014.

[7] Craig R. R. and Bampton M.C.C. Coupling of substructures for dynamic analysis. *AIAA Journal 6*, pages 1313–1319, 1968.